American Journal of Human Genetics, Volume *92*

Supplemental Data

Defective Initiation of Glycosaminoglycan Synthesis due to *B3GALT6* Mutations Causes a Pleiotropic Ehlers-Danlos Syndrome-like Connective Tissue Disorder

Fransiska Malfait, Ariana Kariminejad, Tim Van Damme, Caroline Gauche, Delfien Syx, Faten Merhi-Soussi, Sandrine Gulberti, Sofie Symoens, Suzanne Vanhauwaert, Andy Willaert, Bita Bozorgmehr, Mohamad Hasan Kariminejad, Nazanin Ebrahimiadib, Ingrid Hausser, Ann Huysseune, Sylvie Fournel-Gigleux, and Anne De Paepe

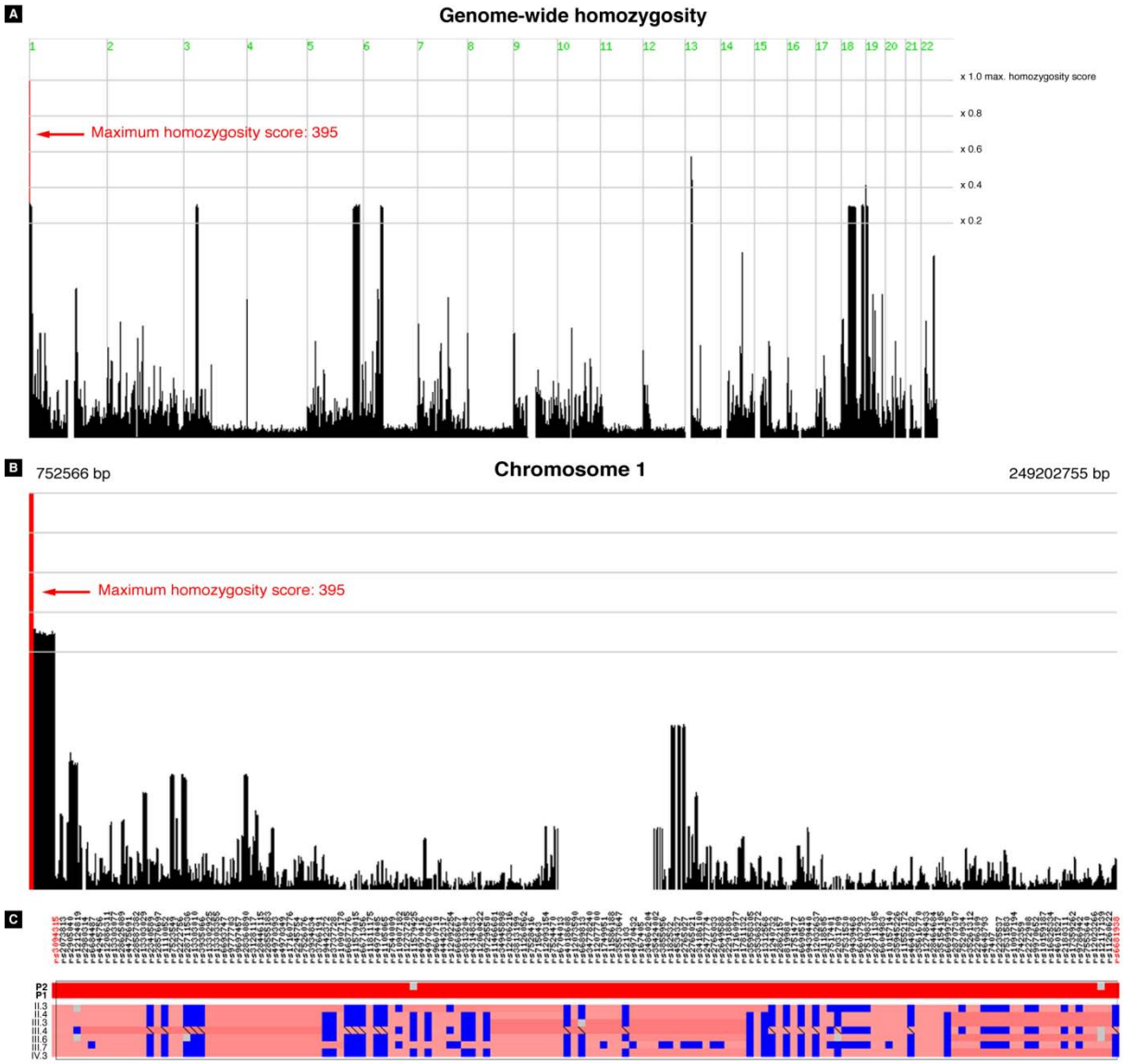

Figure S1. Homozygosity Mapping

Homozygosity mapping in Family 1 revealed a single ~1 Mb region on chromosome 1 (A&B) located between dbSNP rs3094315 and rs6681938 (C). Genomic DNA (gDNA) from individuals P1 and P2 and seven unaffected family members (see Figure 3A for details) was genotyped with the 200K genome-wide Illumina HumanCytoSNP-12 BeadChip SNP array. Homozygosity mapping was performed using the web-based HomozygosityMapper application using recommended default settings.[1] Regions with scores of at least 80% of the maximum homozygosity score were prioritized.

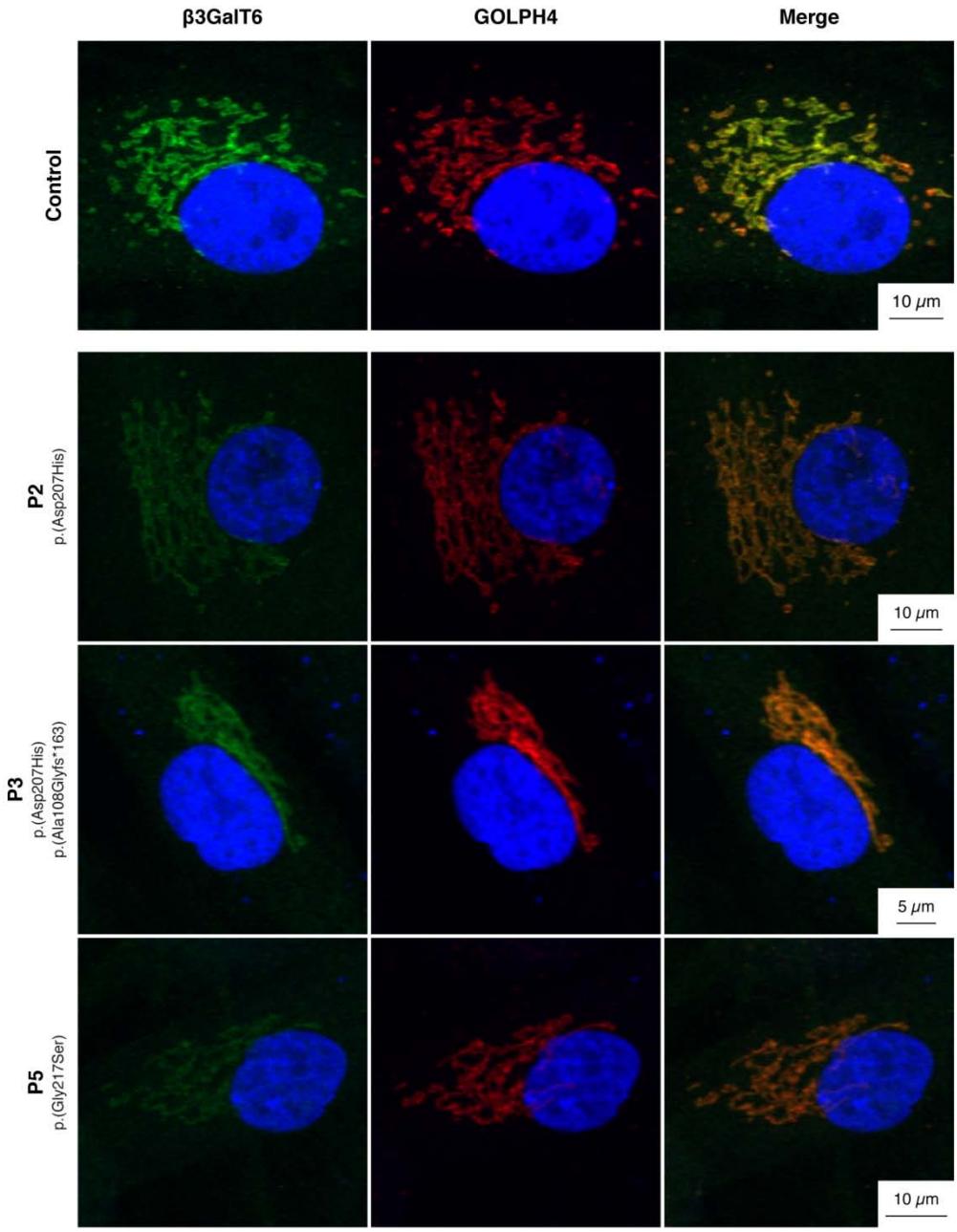

Figure S2. Confocal Immunofluorescence Microscopy of β3GalT6

β3GalT6 (green) co-localises with the Golgi marker GOLPH4 (red). In fibroblasts from P2, P3 and P5, a reduced amount of β3GalT6 protein is observed. Fibroblasts were immunolabeled with anti-β3GalT6 purified MaxPab mouse polyclonal antibody (1:50, Abnova) and rabbit anti-GOLPH4 polyclonal antibody (1:400, Abcam) primary antibodies and subsequently incubated with AlexaFluor488 conjugated goat-anti-mouse (1:1500, Molecular Probes, Life Technologies) and AlexaFluor594 conjugated donkey-anti-rabbit (1:1500, Molecular Probes, Life Technologies) secondary antibodies. Nuclei were counterstained with DAPI (4'-6-diamidino-2-phenylinodole hydroxychloride, Molecular Probes, Life Technologies). Confocal images were captured with a Zeiss LSM780 confocal microscope. Images were taken by using a 63× Pln Apo/1.4 oil objective.

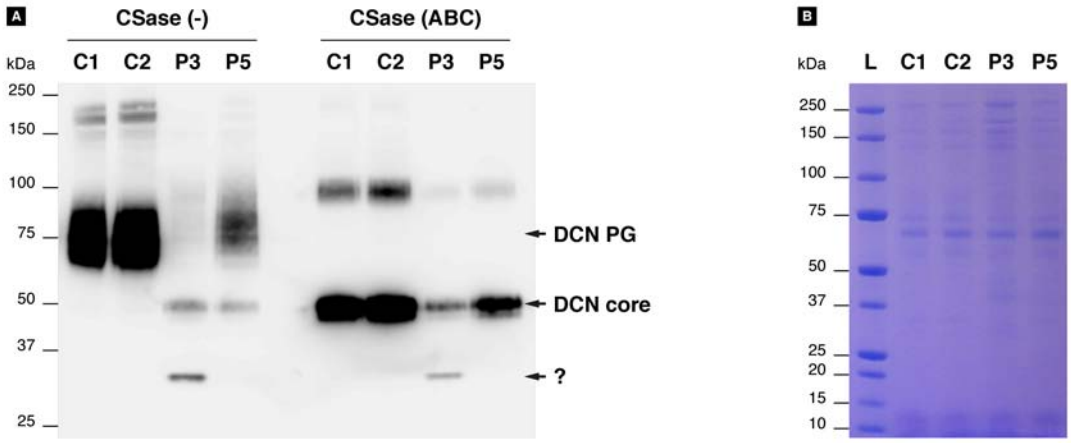

Figure S3. Western Blotting of Decorin Secreted by Cultured Dermal Fibroblasts after Chondroitinase ABC Digestion

(A) In P3 and P5 samples, an additional band (~50 kDa) is observed, migrating with the same molecular mass as the decorin core protein after chondroitinase (CSase) ABC digestion. In addition, the observed amount of decorin core protein is reduced in affected individuals' samples compared to controls. The additional low molecular weight band (~32 kDa) in P3 is probably a degradation product. To perform this analysis, the serum-free conditioned medium from fibroblast cultures was collected at day 7 and concentrated using Centriprep® Centrifugal Filter Devices with Ultracel 30K membranes (Millipore). An aliquot of the concentrated medium was digested with 0.05U of chondroitinase (CSase) ABC from *Proteus vulgaris* (CSase ABC, Sigma-Aldrich). After SDS-PAGE, proteins were transferred to a nitrocellulose membrane using the iBlot® 7-Minute Blotting System, immunolabeled with anti-human decorin antibody (1:250, Clone 115402, R&D Systems) and incubated with horseradish peroxidase (HRP) conjugated goat-anti-mouse secondary antibody (1:5000, Cell Signalling Technologies). Probed membranes were developed using the SuperSignal® West Dura Extended Duration Substrate kit (Thermo Scientific) and scanned with the ChemiDoc-It® 500 Imaging System (UVP). The pre-stained Precision Plus Protein™ All blue Standard (Bio-Rad Laboratories) was used for molecular weight estimation.

(B) To show equal loading, the total protein amount of the concentrated medium was visualized with Imperial™ Protein Stain (Thermo-Scientific) after SDS-PAGE.

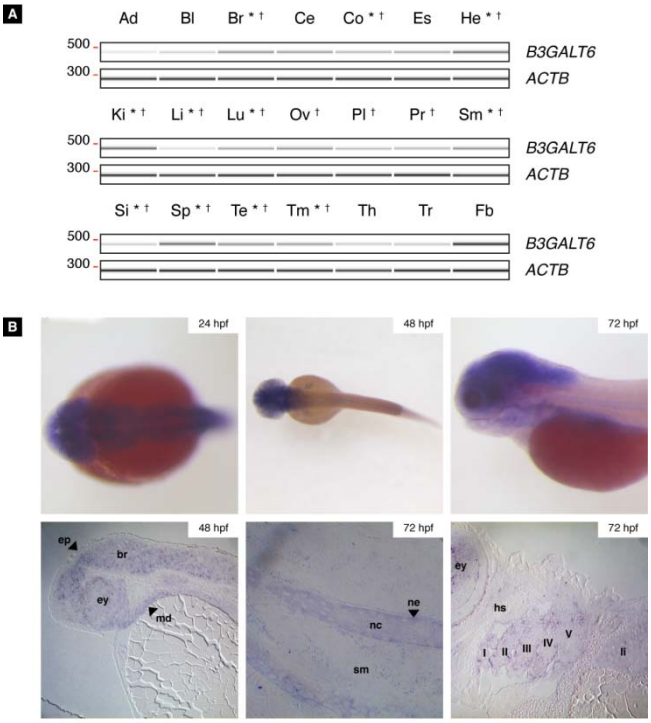

Figure S4. *B3GALT6* Expression in Humans Tissues and Whole-mount *In Situ* Hybridisation of *b3galt6* in Zebrafish Embryos

(A) RT-PCR using the FirstChoice® Human Total RNA Survey Panel covering 20 human tissues (Life Technologies) and pooled RNA from three control human fibroblast cultures reveals ubiquitous *B3GALT6* expression. Tissues examined for *B3GALT6* expression in previous studies are indicated with * [2] and † [3]. Ad: Adipose; Bl: Bladder; Br: Brain; Ce: Cervix; Co: Colon; Es: Esophagus; He: Heart; Ki: Kidney; Li: Liver; Lu: Lung; Ov: Ovary; Pl: Placenta; Pr: Prostate; Sm: Skeletal muscle; Si: Small intestine; Sp: Spleen; Te: Testes; Tm: Thymus; Th: Thyroid; Tr:Trachea; Fb: Fibroblasts.

(B) Whole-mount *in situ* hybridization of zebrafish embryos (24hpf, 48hpf and 72hpf) was performed as previously described [4] and showed expression of *b3galt6* in different tissues including the brain (br), the epithelium of the pharyngeal arches (I-V), cellular layers of the retina (ey, eye), head mesoderm (md), liver (li) and notochord epithelium (ne). The epidermis (ep) and muscle tissue (sm, striated muscle) clearly lacked *b3galt6* expression. Sectioning of whole-mount embryos was performed as previously described. [5] hs: hyosymplectic cartilage.

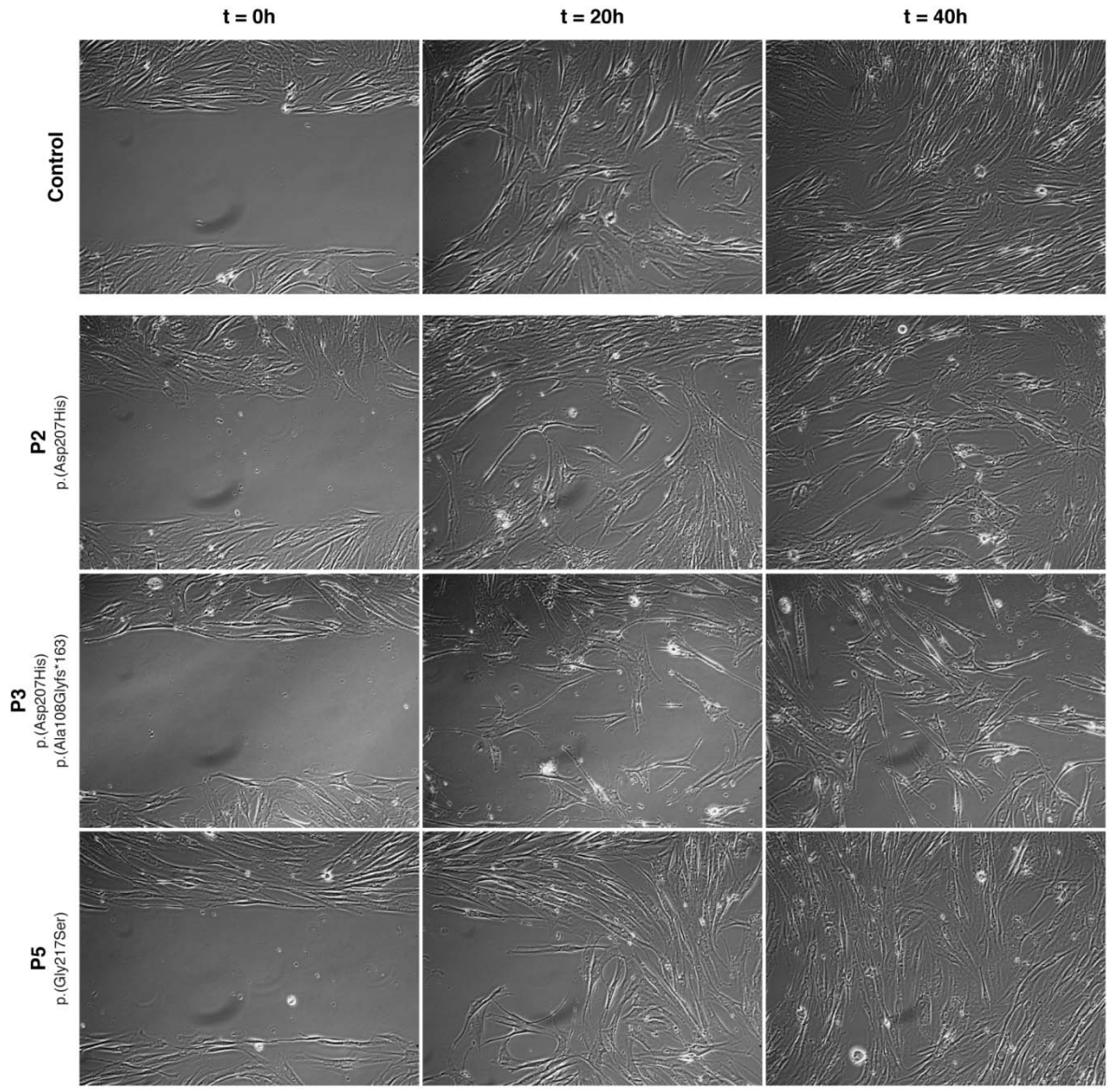

Figure S5. *In Vitro* Wound Closure in Control and β3GalT6-Deficient Fibroblasts

In vitro wound healing assays were performed using silicone inserts (Biovalley) composed of two wells and placed in a 35 mm-diameter Petri dish. Fibroblasts were seeded at 35 x 10^3 cells/well, and the insert was removed at confluency. Cell migration in the denuded area was evaluated by phase-contrast microscopy (magnification 150 x) with a digital camera (Zeiss, AxioCam ERC5S). Representative images of the wound closure are shown at t = 0h, 20h and 40h. Evaluation of the number of migrated cells in the wound area was performed using Photoshop software on a minimum of eight different fields in each group. Wound closure was decreased about 35% and 40% in P2, and by about 65% and 75% in P3, respectively. No difference was observed in P5 compared to control cells.

Table S1. Primer Sequences for Amplification and Bidirectional Sequencing of *B3GALT6* and *DCN*, RT-qPCR and Expression Analysis

Amplicon	Forward sequence	Reverse sequence
Overlapping *B3GALT6* primers for gDNA ampification and bidirectional sequencing		
B3GALT6_Fr1	CTCCGAGGTTGACCAATGAC	GGGCAGGTAGTAGTCGCAGA
B3GALT6_Fr2	CGGACGACGACTCCTTC	CCTTCTCTGGCAGCACT
B3GALT6_Fr3	CAGAGCCTGGAGGACAT	TGAGACGCAGACGTGAGAAA
B3GALT6_Fr4	GTTCCTGGACCTCAGCGA	GAAAGTCTCTTCAGAAAGAAACAATG
B3GALT6_Fr5	TATGTCAGAACTTGGTGCCTGTA	GACAACAAAGACCACAGCG
B3GALT6_Fr6	TCACGTACTTTAACACATCCTTGAA	CGGAGCTCGAACTCAAC
B3GALT6_Fr7	CAGTGGTCTCAGGAGGAAGAAA	TTGGTTCGAATCCCGCT
B3GALT6_Fr8	GTCCCTGCCATCCGATT	TCCAGGTGAGACCAGAGAGA
Primers for RT-qPCR		
B3GALT6	GGAGAGAGTGGTGATCTGT	CTCAACGGCCTGACCTA
DCN	TTTCAATTCCTGAGCTCTTCA	GTGCCCATGAGAATGAGAT
LUM	TGCCAGGAAGAGAGTAAATG	ATTGGTGGATTCTTGTCCAT
HSPG2	TAGAGACGCATCGGAACT	GATGGTGACTTTGACTGTGA
XYLT1	CTGCTCCATGTAGGCATTG	CCTCTGACCTTCTCGAACA
XYLT2	TGGGAAGAAGACTCTGTCAA	CTGAGCTTCAGGCACAATTA
B4GALT7	CACAACTGGGTACAAGACAT	CTTGTCACAGTCCAACATGA
HPRT1	TGACACTGGCAAAACAATGCA	GGTCCTTTTCACCAGCAAGCT
YWHAZ	ACTTTTGGTACATTGTGGCTTCAA	CCGCCAGGACAAACCAGTAT
Primers for expression analysis in human tissues		
B3GALT6	TCACGTACTTTAACACATCCTTGAA	CGGAGCTCGAACTCAAC
ACTB	AGCGAGCATCCCCCAAAGTT	GGGCACGAAGGCTCATCATT

'Fr' and 'Ex' correspond to fragment and the exon number of the amplicons, respectively.

Table S2. *In Silico* Predicion for the Identified Missense Mutations

	SIFT[6-10]		PolyPhen2[11]		MutationTaster[12]	
	Prediction	**Score**	**Prediction**	**Score**	**Prediction**	***p*-value**
c.619G>C p.(Asp207His)	Deleterious	0.02	Probably damaging	1.000	Disease causing	1.0
c.649G>A p.(Gly217Ser)	Deleterious	0.00	Probably damaging	1.000	Disease causing	1.0

Table S3. Comparison of the Clinical Features of β3GalT6-deficient EDS with Other Autosomal Recessive EDS Variants, Autosomal Recessive Cutis Laxa Syndromes and SEMD-JL Type 1

	β3GalT6-deficient	Progeroid[13; 14]	Musculo-contractural[15-17]	EDS VIA[18; 19]	SCD-EDS[20]	FKBP14 deficient[21]	WSS [22]	GO[23]	DBS	SEMD-JL[24]
Inheritance pattern	AR	AR	AR	AR	AR	AR	AR	AR	AR	AR
Gene	*B3GALT6*	*B4GALT7*	*CHST14*	*PLOD1*	*SLC39A13*	*FKBP14*	*ATP6V0A2*	*SCYL1BP1*	*PYCR1*	*Unknown*
Facial characteristics										
Dysmorphic features	(+)	(+)	+ +	-	(+)	-	+	+	+	+
Progeroid, sparse scalp hair	+	+	-	-	-	-	+	+	+	-
Skin										
Skin fragility/ atrophic scars	++	++	++	++	+	(+)	-	-	-	-
Hyperextensibility	+	+	+	+	+	+	-	-	-	+
Bruisability	-	+	+	+	+	-	-	-	-	-
Palmar wrinkling	++	(+)	+	-	(+)	-	++	++	++	+
Generalized cutis laxa	-	-	-	-	-	-	++	-	++	-
Musculoskeletal										
Kyphoscoliosis	++	-	+	+	-	++	+	+	+	++
Joint hyperlaxity	+	+	+	+	+	+	+	+	+	+
Joint contractures	+ progressive	+ ?	++ congenital	-	+ progressive	-	-	-	+	+ progressive ?
Tapering fingers	+	+	+	-	+	-	-	-	-	+
Radioulnar synostosis	-	++	-	-	-	-	-	-	-	(+)
Clubfeet	+	-	+	+	-	(+)	(+)	(+)	+	+
Osteoporosis	++	+	+	+	+	-	+	+	+	+
Spontaneous fractures	++	-	-	-	-	-	-	++	-	-
Skeletal dysplasia	++	+	-	-	+	-	-	-	-	++
Muscle hypotonia	+	(-)	+	+	-	+ +	+	+	+	+

	β3GalT6-deficient	Progeroid [13; 14]	D4ST1 deficient [15-17]	EDS VIA [18; 19]	SCD-EDS [20]	FKBP14 deficient [21]	WSS [22]	GO [23]	DBS	SEMD-JL [24]
Ophtalmological										
Blue sclerae	+	+	+	+	+	(+)	-	-	-	+
Retinal detachment	(+)	-	+	+	-	-	-	-	-	-
Glaucoma/ elevated IO pressure	-	-	+	+	-	-	-	-	+	?
Corneal clouding	-	-	-	-	-	-	-	-	++	(+)

Other										
Mental retardation	++	(+)	-	-	-	-	+	+	++	(+)
Hearing impairment	-	-	(+)	-	-	+	-	-	-	(+)
Gastro-intestinal	-	-	++	-	-	-	-	-	-	-
Genito-urinary	-	-	++	-	-	-	-	-	-	(+)

SCD-EDS: Spondylocheirodysplastic Ehlers-Danlos syndrome; WSS: Wrinkly skin syndrome; GO: geroderma osteodysplasticum; DBS: De Barsy syndrome; SEMD-JL: Spondyloepimetaphyseal dysplasia with joint laxity.

++: Characteristic finding; +: Generally consistent feature; (+): Inconsistent or mild feature; -: Not reported.

Supplemental References

1. Seelow, D., Schuelke, M., Hildebrandt, F., and Nurnberg, P. (2009). HomozygosityMapper--an interactive approach to homozygosity mapping. Nucleic acids research 37, W593-599.

2. Cole, S.E., Mao, M.S., Johnston, S.H., and Vogt, T.F. (2001). Identification, expression analysis, and mapping of B3galt6, a putative galactosyl transferase gene with similarity to Drosophila brainiac. Mammalian genome : official journal of the International Mammalian Genome Society 12, 177-179.

3. Bai, X., Zhou, D., Brown, J.R., Crawford, B.E., Hennet, T., and Esko, J.D. (2001). Biosynthesis of the linkage region of glycosaminoglycans: cloning and activity of galactosyltransferase II, the sixth member of the beta 1,3-galactosyltransferase family (beta 3GalT6). The Journal of biological chemistry 276, 48189-48195.

4. Thisse, C., and Thisse, B. (2008). High-resolution in situ hybridization to whole-mount zebrafish embryos. Nature protocols 3, 59-69.

5. Verstraeten, B., Sanders, E., Huysseune A. . (2012). Whole mount immunohistochemistry and in situ hybridization of larval and adult zebrafish dental tissues. In Odontogenesis Methods and Protocols Methods in Molecular Biology, Kiouss, ed. (USA, Humana Press), pp 887: 179-191.

6. Kumar, P., Henikoff, S., and Ng, P.C. (2009). Predicting the effects of coding non-synonymous variants on protein function using the SIFT algorithm. Nature protocols 4, 1073-1081.

7. Ng, P.C., and Henikoff, S. (2001). Predicting deleterious amino acid substitutions. Genome research 11, 863-874.

8. Ng, P.C., and Henikoff, S. (2002). Accounting for human polymorphisms predicted to affect protein function. Genome research 12, 436-446.

9. Ng, P.C., and Henikoff, S. (2003). SIFT: Predicting amino acid changes that affect protein function. Nucleic acids research 31, 3812-3814.

10. Ng, P.C., and Henikoff, S. (2006). Predicting the effects of amino acid substitutions on protein function. Annual review of genomics and human genetics 7, 61-80.

11. Adzhubei, I.A., Schmidt, S., Peshkin, L., Ramensky, V.E., Gerasimova, A., Bork, P., Kondrashov, A.S., and Sunyaev, S.R. (2010). A method and server for predicting damaging missense mutations. Nature methods 7, 248-249.

12. Schwarz, J.M., Rodelsperger, C., Schuelke, M., and Seelow, D. (2010). MutationTaster evaluates disease-causing potential of sequence alterations. Nature methods 7, 575-576.

13. Bui, C., Talhaoui, I., Chabel, M., Mulliert, G., Coughtrie, M.W., Ouzzine, M., and Fournel-Gigleux, S. (2010). Molecular characterization of beta1,4-galactosyltransferase 7 genetic mutations linked to the progeroid form of Ehlers-Danlos syndrome (EDS). FEBS letters 584, 3962-3968.

14. Quentin, E., Gladen, A., Roden, L., and Kresse, H. (1990). A genetic defect in the biosynthesis of dermatan sulfate proteoglycan: galactosyltransferase I deficiency in fibroblasts from a patient with a progeroid syndrome. Proceedings of the National Academy of Sciences of the United States of America 87, 1342-1346.

15. Dundar, M., Muller, T., Zhang, Q., Pan, J., Steinmann, B., Vodopiutz, J., Gruber, R., Sonoda, T., Krabichler, B., Utermann, G., et al. (2009). Loss of dermatan-4-sulfotransferase 1 function results in adducted thumb-clubfoot syndrome. American journal of human genetics 85, 873-882.

16. Malfait, F., Syx, D., Vlummens, P., Symoens, S., Nampoothiri, S., Hermanns-Le, T., Van Laer, L., and De Paepe, A. (2010). Musculocontractural Ehlers-Danlos Syndrome (former EDS type VIB) and adducted thumb clubfoot syndrome (ATCS) represent a single clinical entity caused by mutations in the dermatan-4-sulfotransferase 1 encoding CHST14 gene. Human mutation 31, 1233-1239.

17. Miyake, N., Kosho, T., Mizumoto, S., Furuichi, T., Hatamochi, A., Nagashima, Y., Arai, E., Takahashi, K., Kawamura, R., Wakui, K., et al. (2010). Loss-of-function mutations of CHST14 in a new type of Ehlers-Danlos syndrome. Human mutation 31, 966-974.

18. Yeowell, H.N., and Walker, L.C. (2000). Mutations in the lysyl hydroxylase 1 gene that result in enzyme deficiency and the clinical phenotype of Ehlers-Danlos syndrome type VI. Molecular genetics and metabolism 71, 212-224.

19. Pinnell, S.R., Krane, S.M., Kenzora, J.E., and Glimcher, M.J. (1972). A heritable disorder of connective tissue. Hydroxylysine-deficient collagen disease. The New England journal of medicine 286, 1013-1020.

20. Giunta, C., Elcioglu, N.H., Albrecht, B., Eich, G., Chambaz, C., Janecke, A.R., Yeowell, H., Weis, M., Eyre, D.R., Kraenzlin, M., et al. (2008). Spondylocheiro dysplastic form of the Ehlers-Danlos syndrome--an autosomal-recessive entity caused by mutations in the zinc transporter gene SLC39A13. American journal of human genetics 82, 1290-1305.

21. Baumann, M., Giunta, C., Krabichler, B., Ruschendorf, F., Zoppi, N., Colombi, M., Bittner, R.E., Quijano-Roy, S., Muntoni, F., Cirak, S., et al. (2012). Mutations in FKBP14 cause a variant of Ehlers-Danlos syndrome with progressive kyphoscoliosis, myopathy, and hearing loss. American journal of human genetics 90, 201-216.

22. Kornak, U., Reynders, E., Dimopoulou, A., van Reeuwijk, J., Fischer, B., Rajab, A., Budde, B., Nurnberg, P., Foulquier, F., Group, A.D.-t.S., et al. (2008). Impaired glycosylation and cutis laxa caused by mutations in the vesicular H+-ATPase subunit ATP6V0A2. Nature genetics 40, 32-34.

23. Hennies, H.C., Kornak, U., Zhang, H., Egerer, J., Zhang, X., Seifert, W., Kuhnisch, J., Budde, B., Natebus, M., Brancati, F., et al. (2008). Gerodermia osteodysplastica is caused by mutations in SCYL1BP1, a Rab-6 interacting golgin. Nature genetics 40, 1410-1412.

24. Beighton, P., and Kozlowski, K. (1980). Spondylo-epi-metaphyseal dysplasia with joint laxity and severe, progressive kyphoscoliosis. Skeletal radiology 5, 205-212.